A simple polarizable model of water based on classical Drude oscillators

Guillaume Lamoureux
Département de physique, Université de Montréal, C.P. 6128, succ. centre-ville, Montréal, Québec, Canada H3C 3J7

Alexander D. MacKerell, Jr.
Department of Pharmaceutical Sciences, University of Maryland, School of Pharmacy, Baltimore, Maryland 21201

Benoît Roux
Department of Biochemistry, Weill Medical College of Cornell University, New York, New York 10021

(Received 14 May 2003; accepted 13 June 2003)

A simple polarizable water model is developed and optimized for molecular dynamics simulations of the liquid phase under ambient conditions. The permanent charge distribution of the water molecule is represented by three point charges: two hydrogen sites and one additional M site positioned along the HOH bisector. Electronic induction is represented by introducing a classical charged Drude particle attached to the oxygen by a harmonic spring. The oxygen site carries an equal and opposite charge, and is the center of an intermolecular Lennard-Jones interaction. The HOH gas-phase experimental geometry is maintained rigidly and the dipole of the isolated molecule is 1.85 D, in accord with experiment. The model is simulated by considering the dynamics of an extended Lagrangian in which a small mass is attributed to the Drude particles. It is parametrized to reproduce the salient properties of liquid water under ambient conditions. The optimal model, refered to as SWM4-DP for ''simple water model with four sites and Drude polarizability,'' yields a vaporization enthalpy of 10.52 kcal/mol, a molecular volume of 29.93 $Å^3$, a static dielectric constant of 79 ± 5, a self-diffusion constant of $(2.30\pm0.04)\times10^{-5}$ cm^2/s, and an air/water surface tension of 66.9 ± 0.9 dyn/cm, all in excellent accord with experiments. The energy of the water dimer is -5.18 kcal/mol, in good accord with estimates from experiments and high level *ab initio* calculations. The polarizability of the optimal model is 1.04 $Å^3$, which is smaller than the experimental value of 1.44 $Å^3$ in the gas phase. It is likely that such a reduced molecular polarizability, which is essential to reproduce the properties of the liquid, arises from the energy cost of overlapping electronic clouds in the condensed phase due to Pauli's exclusion principle opposing induction. © *2003 American Institute of Physics.* [DOI: 10.1063/1.1598191]

I. INTRODUCTION

For meaningful theoretical studies of biomolecular systems, it is necessary to have potential energy functions providing a realistic and accurate representation of both the microscopic interactions and thermodynamic properties. This presents a difficult challenge, particularly when charged or highly polar species are involved (see, e.g., Ref. 1), where electronic polarization is expected to have a significant role in both structure and energetic properties. Current biomolecular potential functions typically account for many-body polarization effects in an average way using an effective parametrization of the atomic partial charges.[2] Because of this approximation, the optimal parametrization is the result of a compromise between an accurate representation of the microscopic energies and bulk solvation properties. Such potential functions can yield meaningful results of semiquantitative accuracy, but are not uniformly reliable under all the solvation conditions relevant to biomolecules. Accordingly, improvements in the representation of biomolecules are anticipated if nonadditive many-body polarization is explicitly taken into account. At the present time, computational chemists and theoreticians are actively pursuing the development of a new generation of force fields for computational studies of biological systems that will include induced polarization.[3,4] However, much more work is needed before such potential functions are ready to be used in simulations of heterogenous biological systems.

Any effort to develop a force field for biomolecular systems must start with a model for water. Water is ubiquitous in biological systems, and a high quality water force field is essential for meaningful simulation studies of biological systems. Many of the models of water currently used in biomolecular simulations are based on fixed effective partial charges which were adjusted to yield accurate bulk liquid properties.[5,6] Although such models, which incorporate the average influence of electronic induction in an isotropic liquid, have been and remain exceedingly useful, there are some well-justified concerns about their ability to represent the properties of liquid in inhomogeneous environments.

Electronic polarization of water is highly sensitive to its environment. In the gas phase, an isolated water molecule has a dipole moment of 1.85 D.[7] However, the average molecular dipole is 2.1 D in the water dimer,[8] increases in larger water clusters,[8] reaching, in the condensed phase, a value

between 2.4–2.6 D, as suggested from classical molecular dynamics simulations of the dielectric properties,[9–11] and 2.95 D, as obtained from *ab initio* molecular dynamics[12,13] and from analysis of experimental data.[14,15] This bulk value is close to the maximum dipole any charged or polar molecule can induce in a water molecule. For instance, adding a sodium ion or a dimethyl phosphate anion to bulk water does not significantly add to the induction effect.[16]

Polarizable water models better reproduce the molecular dipoles in contexts where the hydrogen bonds network of room-temperature bulk water is either partially destroyed or significantly perturbed,[8,17] but, most importantly, they better reproduce the interactions energies. While reproducing the liquid-vapor enthalpy as well as the nonpolarizable models, they have dimer energies closer to -5.0 kcal/mol (the consensus *ab initio* value[18]): -4.69 kcal/mol for the POL3 model,[19] -4.51 kcal/mol for the TIP4P-FQ model,[20] -5.33 kcal/mol for the model of Burnham *et al.*,[17] and -5.00 kcal/mol for the MCDHO model.[21] They adequately reproduce the total binding energy of the water trimer,[17,19,21,22] although the many-body energy contribution itself may be underestimated.

Polarizability appears essential to accommodate the local disruption of the hydrogen bond network created by anions such as chloride[23–27] or fluoride,[28–32] or to reproduce the polarization effects of small multivalent cations on the first hydration shell.[33,34] And although explicit polarizability does not appear to have any significant effect on the reorganization of water molecules at flat liquid–hydrophobic,[35] liquid–vapor,[19,36] or liquid–metal[37,38] interfaces, it may play a decisive role for the specific water–water interactions near small nonpolar moieties.[39,40] In short, polarizability is essential to get from the same water model accurate energetics in the vicinity of highly polar moieties (such as carbonyl groups), small ions (such as sodium or chloride), as well as in anisotropic nonpolar environments.

Although a polarizable water model based on a simple potential may not capture the delicate energy balance needed to describe all phase transformations accurately from ice to water vapor, it should considerably help in increasing the accuracy of biomolecular simulations, which are largely generated around ambient conditions of pressure and temperature. It is important to continue to search for simple models of water that are accurate and computationally inexpensive, and that are adapted to investigate problems in large complex biomolecular systems, which requires very long simulation times. That said, it is important to keep in mind that even an *exact* microscopic potential function might not automatically lead to accurate thermodynamic properties in classical simulations, which neglect the quantum nature of the nuclei. For example, there are clear, albeit small, differences between classical and quantum simulations of the bulk liquid based on a given water model.[41] For this reason, parametrization of the potential function is unavoidable to reproduce macroscopic properties accurately.

The goal of the present paper is to present a simple model for water and determine its optimal parametrization. In this model, a water molecule is represented as a rigid object imposing the experimental gas phase molecular geometry, with four interaction sites: the oxygen, carrying the molecular polarizability but no net charge, the two hydrogens, and an additional site located along the HOH bisector. An isotropic polarizability is introduced by adding a charged mobile auxiliary particle attached to the oxygen by a harmonic spring: a classical Drude oscillator.[42]

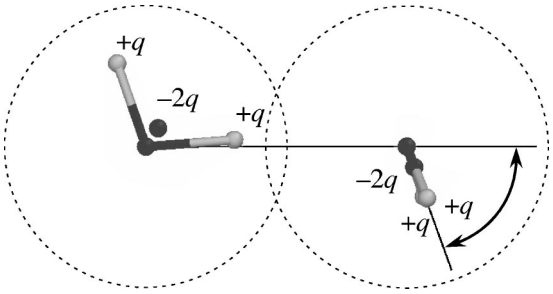

FIG. 1. Illustration of the SWM4-DP water dimer. The molecular structures are shown as ball-and-stick models, with separate M sites. The Drude particles are too close to the oxygen sites to be shown. The arrow defines the acceptor angle θ_A.

Many polarizable models of comparable complexity exist in the literature. Some of the most recent (and most successful) are the RPOL model of Dang,[43] the TIP4P-FQ model of Rick *et al.*,[20] the BSV model of Brodholt *et al.*,[44] the ''polarizable point-charge'' (PPC) model of Svishchev *et al.*,[45] the POL model of Dang and Chang,[19] the MCDHO model of Saint-Martin *et al.*,[21] the shell water (SW) models of van Maaren and van der Spoel,[46] the POL5 models of Stern *et al.*,[47] and the ''charge-on-spring'' (COS) models of Yu *et al.*[48] Most of these models significantly overestimate the static dielectric constant ϵ of liquid water. Typically, ϵ is higher than 100, compared to the expected value of 78.4.[49] Such an incorrect electrostatic shielding is an important shortcoming for a model to be used as a solvent for biomolecules. Only TIP4P-FQ and PPC models have ϵ close to 80. But they have electrostatic representations that may be considered limiting: their out-of-plane molecular polarizability components are zero,[20,45] whereas the molecular polarizability of water is almost isotropic.[50]

The model presented in this work is adjusted to reproduce the potential energy, density, self-diffusion constant, and static dielectric constant of bulk liquid water under normal temperature and pressure conditions, using the double-thermostat molecular dynamics algorithm described previously.[51] Simply by reproducing these four bulk properties, we find a consistent microscopic picture: good dimer energy and good hydrogen-bonding geometry, as well as consistent energies for water clusters.

II. THEORY AND METHODS

A. Model and computational details

The model considered here is closely related to the TIP4P model.[5] The water molecule is kept in a fixed geometry, with four interaction sites: the oxygen and hydrogen atoms and an additional massless site, called ''M,'' located at a fixed distance ℓ_{OM} along the bisector of the HOH angle (see Fig. 1). The oxygen and hydrogen atoms are kept in the

experimental geometry of the water molecule in the gas phase with a OH bond length of 0.9572 Å and a HOH angle of 104.52°.[52] A mobile auxiliary particle, a classical Drude oscillator,[42] is attached by a harmonic spring of force constant k_D to the oxygen site to represent induced polarizability.[51] The Drude particle carries a positive charge q_D while the oxygen carries a charge $-q_D$. During dynamics, the Drude particle stays near the minimum energy position, $\mathbf{r}_O + q_D\mathbf{E}/k_D$, where $\mathbf{E}$ is the field arising from the surrounding molecules. The displacement of the Drude particle gives rise to an induced dipole, $q_D^2\mathbf{E}/k_D$. Correspondingly, the molecular polarizability α is equal to q_D^2/k_D.[51] The permanent dipole of the isolated molecule in the gas phase is set by the charge carried by the hydrogen atoms and the massless interaction site M; the charge on the hydrogens is $q_H = q$ and the the charge on M is $q_M = -2q$.

Unshielded $1/r$ Coulombic potentials are assumed between all the intermolecular pairs of interaction sites s (O, H1, H2, M, and D) and the core repulsion and nonpolar interactions are represented using a Lennard-Jones "12-6" potential between each oxygen–oxygen (OO) pair. The total potential energy for a system of water molecules is

$$U_{\mathrm{tot}}(\{\mathbf{r}\}) = \sum_i \frac{1}{2} k_D |\mathbf{r}_{O,i} - \mathbf{r}_{D,i}|^2 + \sum_{i<j} \sum_{s,s'} \frac{q_s q_{s'}}{|\mathbf{r}_{s,i} - \mathbf{r}_{s',j}|} + \sum_{i<j} 4\epsilon_{OO}\left[\left(\frac{\sigma_{OO}}{|\mathbf{r}_{O,i} - \mathbf{r}_{O,j}|}\right)^{12} - \left(\frac{\sigma_{OO}}{|\mathbf{r}_{O,i} - \mathbf{r}_{O,j}|}\right)^{6}\right]. \quad (1)$$

The model is very simple and has only a few parameters which need to be optimized: the length ℓ_{OM} between the oxygen and the M site, the charge q, the spring constant k_D and the charge of the Drude particle, q_D, and the coefficients of the Lennard-Jones potential ϵ_{OO} and σ_{OO}. In fact, the model is highly constrained and there are only four independent parameters: ℓ_{OM}, α, ϵ_{OO}, and σ_{OO}. All the other parameters can be deduced directly. The magnitude of the charge q on the M site is constrained so that the total permanent dipole for an isolated molecule, $\mu_0 = 2q[\ell_{OH}\cos(\frac{1}{2}\theta_{HOH}) - \ell_{OM}]$, matches the experimental gas phase value of 1.85 D.[7] Furthermore, as long as the spring constant k_D is sufficiently large, the point-dipole approximation is valid and only the combination q_D^2/k_D, corresponding to the polarizability α, is a free parameter. Within this approximation, the sign of the charge carried by the Drude particle is irrelevant, and we chose arbitrarily q_D to be positive. We use a spring constant of 1000 kcal/mol/Å^2, which insures that the point-dipole limit is valid.[51] The four parameters of the model are optimized to match a number of properties as accurately as possible according to the procedure described in the next section.

B. Parametrization strategy

We seek to optimize the parameters of the model to reproduce the vaporization enthalpy, density, static dielectric constant, and self-diffusion constant in the liquid phase at ambient conditions of pressure and temperature. The ability of the model to reproduce the radial distribution functions from experiments[53,54] is monitored, as a final criteria, though it is not used directly in the optimization procedure. The following parameters have to be adjusted: ℓ_{OM}, α, ϵ_{OO}, and σ_{OO}. In fact, for given values of ℓ_{OM} and α, it is possible to adjust the Lennard-Jones parameters ϵ_{OO} and σ_{OO} to get specific values of the interaction energy U_{dimer} and the oxygen–oxygen equilibrium distance d_{OO} of the optimized water dimer. In seeking to characterize different models in terms of the average properties of the bulk liquid, we found it more practical to use those quantities directly, instead of the Lennard-Jones parameters ϵ_{OO} and σ_{OO}. The main advantage is that they are more directly related to the vaporization enthalpy and density of the liquid than the Lennard-Jones parameters, thus making the parameter search easier to interpret. Since there is a one-to-one correspondence between $(\epsilon_{OO}, \sigma_{OO})$ and $(U_{\mathrm{dimer}}, d_{OO})$ in the range of interest, this choice does not limit the number of possible models.

The overall parametrization strategy is the following: First, a large number of models with different values of ℓ_{OM}, α, U_{dimer}, and d_{OO} were generated in order to explore the parameter space and determine the region yielding reasonable values for the average molecular volume $\langle v \rangle$, interaction energy Δu, self-diffusion constant D, and static dielectric constant ϵ. In the following stage, a "grid" search is set up to explore the properties of the model by varying the four parameters systematically. A $3\times3\times4\times3$ grid was used (three values for ℓ_{OM}, α, and d_{OO}, and four values for U_{dimer}), corresponding to a total of 108 simulations. Then, a quadratic polynomial response-surface model $\mathbf{P}$ was fitted to the results of the 108 simulations to provide an interpolation formula predicting the liquid properties for any parametrization within the grid without having to actually perform the simulation. From the polarizability α, the ℓ_{OM} distance, and the energy U_{dimer} and oxygen–oxygen distance d_{OO} for the water dimer, the response function $\mathbf{P}$ provides predicted values for Δu, $\langle v \rangle$, height of the first peak in the oxygen–oxygen radial distribution function, $g_{OO}^{(1)}$, and average dipole $\langle \mu \rangle$:

$$\{\Delta\hat{u}, \langle\hat{v}\rangle, \hat{g}_{OO}^{(1)}, \langle\hat{\mu}\rangle\} = \mathbf{P}(\alpha, \ell_{OM}, U_{\mathrm{dimer}}, d_{OO}). \quad (2)$$

(The hat is to distinguish the predicted values from the actual values one would get from performing the simulation.) The coefficients of the response function are determined using a least-squares fit. There are 15 coefficients for each property for a total number of 60 coefficients. Such a polynomial response function can be formally inverted ($\mathbf{P}^{-1}$) to get the parameters that produce some chosen values for $\hat{g}_{OO}^{(1)}$ and $\langle\hat{\mu}\rangle$ while satisfying the conditions $\langle\hat{v}\rangle = 29.94$ Å^3 (corresponding to a density of 0.0334 molecules/Å^3) and $\Delta\hat{u} = -9.92$ kcal/mol. In the final stage, the parameters were adjusted to reproduce the experimental values for Δu and $\langle v \rangle$, and to obtain good agreement for D and ϵ.

C. Computational details

All simulations were performed by considering the dynamics of an extended Lagrangian in which a small mass m_D and kinetic energy is attributed to the Drude particles. The amplitude of their oscillations away from the local en-

ergy minimum is controlled with a low-temperature thermostat acting in the local center-of-mass reference frame of each oxygen–Drude pair.[51] The Drude particle is attached to the oxygen with a harmonic spring with a force constant k_D of 1000 kcal/mol/Å^2. Its mass is set to 0.4 amu and the mass of the oxygen is set to 15.5994 amu, such that the total mass of the oxygen–Drude pair is equal to 15.9994 amu (the correct mass of an oxygen atom). To ensure that the time course of the induced dipoles stays close to the self-consistent-field (SCF) solution, a Nosé–Hoover thermostat at a temperature $T_\star = 1$ K is applied to the relative motion of each oxygen–Drude pair (in their local center-of-mass reference frame). The relaxation time of the Drude oscillator thermostat at temperature $T_\star$ is 0.005 ps (5 fs). It was previously shown that the trajectories generated according to this procedure are very close to those generated by the SCF regime of induced polarization.[51] To control the global thermalization of the system, a second Nosé–Hoover thermostat at room temperature T is applied to the center-of-mass of the oxygen–Drude pairs as well as the hydrogens atoms. A modified Andersen–Hoover barostat is used to maintain the system at constant pressure P of 1 atm.[51,55] A relaxation time of 0.1 ps is assigned to the barostat, which, combined with the global thermostat, maintains the system at ambient conditions of pressure and temperature. The water molecules are constrained to the experimental geometry using the SHAKE/Roll and RATTLE/Roll procedures.[56] At each dynamical step, the total force acting on the massless M sites is redistributed onto the oxygen and hydrogen atoms and their position is geometrically reconstructed after each move. The trajectory is propagated with a 1.0 fs time step, using a multistep integration procedure for the thermostat variables.[51] This modified two-temperature isobaric–isothermal ensemble, or $NP(T,T_\star)$ ensemble, is a variant of the isobaric-isothermal equations of Martyna *et al.*[55] and has been implemented in the biomolecular program CHARMM.[57] See Ref. 51 for further detail.

Systems of 250 water molecules were simulated with cubic periodic boundary conditions. The electrostatic interactions were treated without truncation using particle-mesh Ewald (PME) summation[58] (with $\kappa = 0.33$ for the charge screening and fourth-order splines for the mesh interpolations) and a 15 Å cutoff for the Lennard-Jones interactions. Some of the exploratory simulations were performed using smaller boxes (125 molecules) and smaller cutoffs (9 Å) for the Lennard-Jones interactions. Each box was simulated for 150 ps and the average liquid properties were extracted from the last 100 ps. For each simulation, the average molecular volume $\langle v \rangle$ and the vaporization enthalpy Δh are calculated and compared with the experimental values. The correct target values are 29.94 Å^3 for the molecular volume (corresponding to 0.997 g/cm^3) and 10.52 kcal/mol for the vaporization enthalpy.[59] Under the constant pressure simulation conditions, the average molecular volume $\langle v \rangle$ is extracted directly from the average volume $\langle V \rangle$ of the periodic simulation box. The vaporization enthalpy Δh is calculated from the average net gain of potential energy Δu upon formation of the dense system

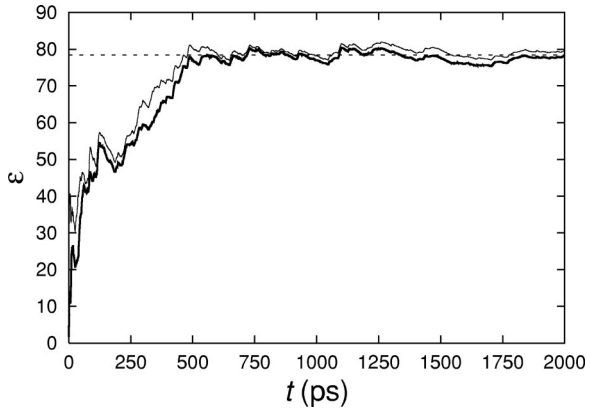

FIG. 2. Convergence of the dielectric constant as $\mathbf{M}(t)$ is accumulated [see Eq. (4)]. $\mathbf{M}(t)$ is the concatenation of the 20 100 ps time series. The thin line corresponds to Eq. (4) assuming $\langle \mathbf{M} \rangle = 0$ by symmetry. The fine horizontal line shows the experimental value $\epsilon = 78.4$ (Ref. 49).

$$\Delta h = k_B T - \Delta u = k_B T - (\langle u \rangle_{\text{liq}} - \langle u \rangle_{\text{gas}}) = k_B T - (\langle u \rangle_{\text{liq}} - \tfrac{3}{2} k_B T_\star). \tag{3}$$

It should be noted that, even though the water molecules themselves are rigid, the thermal contribution from the Drude oscillators to the total potential energy, $\frac{3}{2} k_B T_\star$, must be subtracted in an extended Lagrangian simulation (even though this correction is small for $T_\star = 1$ K). Practically, Δu rather than Δh is considered in the analysis. The average structure of the liquid was characterized by calculating the oxygen–oxygen, oxygen–hydrogen, and hydrogen–hydrogen radial distribution functions, $g_{\text{OO}}(r)$, $g_{\text{OH}}(r)$, and $g_{\text{HH}}(r)$, and compared with experiments.[53,54] The dielectric constant of the liquid ϵ was calculated using,[60]

$$\epsilon = \epsilon_\infty + \frac{4\pi}{3\langle V \rangle k_B T} (\langle \mathbf{M}^2 \rangle - \langle \mathbf{M} \rangle^2), \tag{4}$$

where $\mathbf{M}$ is the total dipole moment of the box and ϵ_∞ is estimated from the Clausius–Mossotti equation (see, e.g., Ref. 61):

$$\frac{\epsilon_\infty - 1}{\epsilon_\infty + 2} = \frac{4\pi}{3} \frac{\alpha}{v}. \tag{5}$$

The convergence of ϵ is monitored by plotting its value as the time series, $\mathbf{M}(t)$, is accumulated (see Fig. 2). It is also useful to monitor the average molecular dipole $\langle \mu \rangle$ because it is strongly correlated with the dielectric constant even though its convergence is an order of magnitude faster than Eq. (4). The Debye relaxation time τ_D was extracted from the first 40 ps of the exponential decay of the dipole time autocorrelation function,[62]

$$\Phi(t) = \frac{\langle \mathbf{M}(t) \cdot \mathbf{M}(0) \rangle}{\langle \mathbf{M}^2 \rangle}. \tag{6}$$

The self-diffusion constant D was calculated from the mean squared displacement,[63]

$$D = \lim_{t \to \infty} \frac{1}{6t} \left\langle \frac{1}{N} \sum_{i=1}^{N} [\mathbf{r}_{\text{O},i}(t) - \mathbf{r}_{\text{O},i}(0)]^2 \right\rangle. \tag{7}$$

The self-diffusion constant D and static dielectric constant ϵ are computed from ten independent simulations of 150 ps, using the same initial conformation but assigning different random initial velocities. The uncertainty on both ϵ and D are estimated from the spread of the values for the ten independent simulations. The properties of the final model are further converged using ten additional independent simulations.

As an additional validation of the optimal model, interfacial properties were characterized by calculating the air/water surface tension γ, and the interfacial electrostatic potential $\Delta\phi$. A system of 250 water molecules was simulated in a slab geometry in a 19.56 Å$\times$19.56 Å$\times$58.68 Å tetragonal periodic cell. The surface tension γ is computed from the pressure increase perpendicular to the interface,[64]

$$\gamma = \tfrac{1}{2} L_z [\langle P_{zz} \rangle - \tfrac{1}{2}(\langle P_{xx} \rangle + \langle P_{yy} \rangle)], \tag{8}$$

where $L_z = 58.68$ Å. The volume of the system was kept constant and the pressure tensor was monitored. The interfacial potential was calculated from the average electrostatic potential along the z axis, $\phi(z)$, obtained by integrating the charge density $\rho(z)$:

$$\phi(z) = -\frac{4\pi}{\epsilon_0} \int_{-\infty}^{z} dz' \left[\int_{-\infty}^{z'} dz'' \, \rho(z'') - \int_{z'}^{\infty} dz'' \, \rho(z'') \right]. \tag{9}$$

Five independent simulations were equilibrated for 100 ps and data was accumulated for an additional 1000 ps. Last, to assess how the optimal model reproduces the energetics and the geometry of hydrogen bonding, we examined the binding energies of small water clusters (trimer, tetramer, pentamer, and hexamer).

III. RESULTS AND DISCUSSION

A. Optimal parametrization

For the sake of simplicity, we chose a rigid model imposing the experimental geometry of the water molecules in the gas phase. The permanent molecular dipole is created by partial charges on the hydrogen atoms and on a nonatomic M site positioned along the HOH bisector. An isotropic polarizability is attributed exclusively to the oxygen site by a classical Drude oscillator (site D). Site D has a positive charge, matched by a negative charge on the oxygen site. The total potential energy is represented by simple radial functions as expressed in Eq. (1).

In several ways, the current model is exceedingly simple, and this has important consequences. In particular, the model does not account for obvious factors such as the flexibility of the water molecule and the small increase in the OH bond length and in the HOH bond angle, known to occur in the liquid.[65] Furthermore, nuclear quantum effects giving rise to zero point vibration, which can be substantial because of the light mass of the hydrogen nuclei, are completely ignored. It is therefore unrealistic to expect that the model be able to provide a correct representation of the all properties of water, going all the way from small systems (monomer, dimer, trimer) up to dense bulk phases (liquid, solid) under a variety of conditions of temperature and pressure. The optimal parametrization of the current model reflects a compromise that is aimed at the most relevant situations for biomolecular systems. Thus, where to make compromises becomes an important issue. Widely used effective potentials, with no induced polarizability, were parametrized to quantitatively match the enthalpy and density of the liquid as correctly as possible. These models often have tolerated fairly large inaccuracies in the representation of small clusters. For example, the permanent dipole of effective nonpolarizable water models deviates significantly from the dipole of an isolated water molecule in the gas phase. The experimental dipole is 1.85 D whereas it is 2.35 D for TIP3P,[5] 2.27 D for SPC,[6] and 2.18 D for TIP4P.[5] The dipole of these models was enhanced to yield better thermodynamic properties for the liquid phase. Similarly, these models significantly overestimate the interaction energy of the water dimer by 1 to 1.5 kcal/mol. Nonetheless, effective nonpolarizable models have displayed a remarkable ability to describe biomolecular systems under ambient conditions semiquantitatively.[66] This observation carries an important message for the development of novel polarizable force field; even though it is important to have as good a representation of the small systems as possible, it is, first and foremost, essential to reproduce the basic thermodynamic properties of the bulk phase. Therefore, it seems reasonable to accept small deviations for the small systems if this allows for reproduction of the thermodynamic properties. Furthermore, it is also important to realize that there are often uncertainties about the ''correct'' target values, particularly in the case of small clusters. For example, the interaction energy of the water dimer is -5.4 ± 0.7 kcal/mol from experimental measurements,[67,68] but is -5.0 ± 0.1 kcal/mol, according to high-level *ab initio* calculation.[18] Such variations are small, but can nonetheless have an important impact on the properties of the condensed phase. Therefore, models which yield a dimer energy anywhere around the estimates from *ab initio* or gas phase experiments are acceptable and should be tested.

Even though the magnitude of the polarizability α of an isolated water molecule in the gas phase is 1.44 Å^3, in the bulk phase it is likely that molecular polarization is opposed by the energetic cost arising from Pauli's exclusion principle due to the overlap of neighboring electronic charge distributions.[69] This phenomena is accounted for by a ''renormalized'' effective α in the liquid that is smaller than the gas phase value. Recent *ab initio* calculations on the water dimer[70] and on small water clusters[71,72] suggest that the condensed phase molecular polarizability can be 7% to 9% less than in gas phase. In the present work, the need for a smaller polarizability to reproduce the properties of the liquid phase became apparent from a large number of simulations (several hundred) exploring many models over a wide range of the three parameters ℓ_{OM} (between 0.0 and 0.35 Å), U_{dimer} (between -5.5 and -4.5 kcal/mol), and d_{OO} (between 2.7 and 3.0 Å) while keeping α at 1.44 Å^3. From this large number of simulations, it was clear that models with the experimental gas-phase polarizability systematically yield an overestimated dielectric constant, typically in the range of 150 to 200. Furthermore, none of these models could get both the correct density and enthalpy: liquid densities close to the experimental value always resulted in a

vaporization enthalpies that were too favorable by about 1 to 2 kcal/mol. The average dipole of those models is around 2.9 D, which is consistent with the overestimated dielectric constant.[9] (For similar water models having a simple electrostatic representation based on unified atomic charges and polarizabilities, a dielectric constant in the correct range requires an average dipole between 2.4 and 2.6 D.[9–11]) On the basis of these observations, the molecular polarizability α was then treated as an empirical adjustable parameter in optimizing the model. Models with values of α varying between 0.6 to 1.4 Å^3 were simulated. The results clearly indicated that the value of α must be around 1.0 Å^3 to yield reasonable liquid properties.

Once the reasonable range of the four parameters was established, the properties of different models were explored by a systematic grid search procedure. A total of 108 models were simulated with all combinations of the following parameter values: $\ell_{OM}=0.23$, 0.24, 0.25 Å; $\alpha=0.95$, 1.00, 1.05 Å^3; $U_{OO}=-5.4$, -5.3, -5.2, -5.1 kcal/mol; and $d_{OO}=2.81$, 2.82, 2.83 Å. The polynomial response function **P** of Eq. (2) was fitted to the results of the simulations and numerically inverted to help determine the optimal parameters for the model. As long as the models are kept within the range of parameters that were actually explored by the simulations, the polynomial prediction turned out to be very accurate, even more reliable than a single simulation, because the random statistical errors of individual simulations are filtered out by the fitting procedure. In the final stage of refinement, the strong correlation between the average molecular dipole in the liquid and the dielectric constant, as well as the strong correlation between the height of the first peak in the oxygen–oxygen radial distribution function and the diffusion constant, were exploited to converge more rapidly towards an optimal model. Assuming that everything else remains the same, the self-diffusion constant decreases when the first peak is enhanced. Within the constraints of the current model, it is possible to have an acceptable self-diffusion constant only if the maximum of the first peak is close to 3.0. Similarly, the dielectric constant increases when the average dipole per molecule in the liquid is increasing. An acceptable dielectric constant is produced only if the average dipole is around 2.45 D, within a narrow range. For example, a model, whose parameters were chosen via $\mathbf{P}^{-1}$ to impose a maximum in the radial distribution function $g_{OO}^{(1)}$ of 3.00 Å and an average dipole $\langle\mu\rangle$ of 2.44 D, yields a diffusion constant D of 2.38×10^{-5} cm^2/s and a dielectric constant ϵ equal to 79 ±10. A closely related model, whose parameters were chosen to impose $g_{OO}^{(1)}=3.05$ Å yields $D=2.17\times10^{-5}$ cm^2/s but $\epsilon=71\pm10$. Combining this information, four more models were simulated with parameters chosen to yield $g_{OO}^{(1)}=3.05$ Å, and an average dipole $\langle\mu\rangle$ equal to 2.445, 2.450, 2.455, and 2.460 D. The results were 2.27, 2.24, 2.29, and $(2.21\pm0.07)\times10^{-5}$ cm^2/s for the diffusion constant, and 74, 79, 79, 82 ± 10 for the dielectric constant. The third (and best) model was chosen. Table I shows the final set of parameters and Table II the liquid properties. We call this optimized model SWM4-DP, standing for ''simple water model (4-site) with Drude polarizability.''

We obtain better converged properties for the SWM4-DP model by performing ten additional independent simulations. With a total of 20 simulations, the diffusion constant is $(2.30\pm0.04)\times10^{-5}$ cm^2/s and the dielectric constant is 79 ± 5. The convergence of the dielectric constant is shown in Fig. 2. For the SWM4-DP model, the Clausius–Mossotti equation (5) gives $\epsilon_\infty=1.52$. A more direct estimation of ϵ_∞ can be obtained by computing the dielectric contribution of the dipole fluctuations for many frozen nuclear configurations,

$$\epsilon_\infty=1+\frac{4\pi}{3\langle V\rangle_{(f)}k_BT_\star}(\langle\mathbf{M}^2\rangle_{(f)}-\langle\mathbf{M}\rangle_{(f)}^2), \tag{10}$$

where $\langle\cdots\rangle_{(f)}$ indicates an average over induced-dipole fluctuations only. This average is obtained for Drude oscillators moving according to Langevin dynamics at temperature $T_\star$ and for all nuclei frozen in a configuration extracted from the molecular dynamics. Equation (10) exploits the fact that, under a linear response theory, the classical fluctuations of the induced dipoles are a direct measure of the total polarizability A of the box. This treatment is equivalent to the approach of Neumann and Steinhauser.[60] The temperature of the Langevin simulation is irrelevant and gives almost identical results whether $T_\star=1$ K or 300 K. Averaging ϵ_∞ for ten uncorrelated nuclear conformations gives $\epsilon_\infty=1.68$ for the SWM4-DP model, a value that is slightly higher than the mean-field estimate predicted by the Clausius–Mossotti equation (1.52) but lower than the experimental estimate (1.79).[61]

It is of interest to examine the sensitivity of the parameters in the context of a given model. Figure 3 shows some projections of the response surface **P**. It is observed that the interaction energy of the water dimer, U_{dimer}, and the oxygen–oxygen equilibrium distance d_{OO} have almost opposite effects on the average molecular energy Δu and volume $\langle v\rangle$ in the liquid. Generating different models with variations only in these two quantities, which are closely related to the parameters of the Lennard-Jones potential, ϵ_{OO} and σ_{OO}, is a very inefficient way to span the $\langle v\rangle-\Delta u$ plane. These figures show why models with inappropriate values for α and ℓ_{OM} cannot be ''fixed'' by adjusting U_{dimer} and d_{OO}: They would require unphysical values of U_{dimer} and d_{OO}, that would

TABLE I. Parameters of the SWM4-DP water model compared to the TIP3P model. For SWM4-DP, ℓ_{OM}, $q_D=-q_O$, ϵ, and σ_{OO} were adjusted to reproduce the liquid properties.

	TIP3P[a]	SWM4-DP[b]
ℓ_{OH} (Å)	0.9572	0.9572
θ_{HOH} (°)	104.52	104.52
ℓ_{OM} (Å)		0.238 08
q_O (e)	−0.834	−1.771 85
q_M (e)		−1.107 40
q_H (e)	0.417	0.553 70
q_D (e)		1.771 85
k_D (kcal/mol/Å^2)		1000
ϵ_{OO} (kcal/mol)	0.1521	0.205 68
σ_{OO} (Å)	3.1506	3.180 30

[a]From Ref. 5.
[b]This work.

TABLE II. Parameters and properties of a selection of water models. The components of the traceless quadrupole Q are defined using the MO direction as x axis, the H_1H_2 direction as y axis, and the perpendicular direction as z axis.

	Expt.[a]	TIP3P[b]	RPOL[c]	TIP4P-FQ[d]	POL[e]	MCDHO[f]	SW-RIGID[g]	POL5/TZ[h]	COS/B2[i]	SWM4-DP[j]
ℓ_{OH} (Å)	0.9572	0.9572	1.0000	0.9572	0.9572	0.9590	0.9572	0.9572	1.0000	0.9572
θ_{HOH} (°)	104.52	104.52	109.50	104.52	104.52	104.83	104.52	104.52	109.47	104.52
ℓ_{OM} (Å)				0.15	0.215		0.1374			0.238 08
μ_0 (D)	1.85	2.347	2.024	1.85	1.848	1.85	1.85	1.854	2.07	1.85
α (Å^3)	1.44		1.47	1.123	1.444	1.352	1.47	1.291	0.93	1.042 52
Q_{xx} (DÅ)	−0.134	−0.080	−0.263	−0.098	−0.188	−0.24	−0.13	−0.002	−0.27	−0.2421
Q_{yy} (DÅ)	2.626	1.762	1.885	1.882	2.235	2.67	2.63	2.337	1.93	2.4068
Q_{zz} (DÅ)	−2.493	−1.681	−1.623	−1.785	−2.047	−2.44	−2.50	−2.335	−1.66	−2.1647
U_{dimer} (kcal/mol)	−5.4	−6.50	−5.5	−4.5	−4.69	−5.00	−5.24	−4.96	−5.57	−5.18
d_{OO} (Å)	2.98	2.74	2.82	2.92	2.87	2.92	2.93	2.896	2.79	2.82
θ_A (°)	58	20		27		56	56	63	51	70
μ_{dimer} (D)	2.643	3.866		3.430	2.05	2.681	2.47	2.435	3.76	2.087
Δu (kcal/mol)	−9.92	−9.82	−9.94	−9.9	−9.84	−10.40	−9.96	−9.92	−9.97	−9.927
$\langle v \rangle$ (Å^3)	30.0	29.9	30.1	30.0	30.1	29.33	30.04	30.00	30.1	29.93
$\langle \mu \rangle$ (D)		2.35	2.62	2.62	2.75	3.01	2.61	2.712	2.62	2.456
D (10^{-5} cm^2/s)	2.3	5.1	2.4±0.3	1.9	2.1±0.1		3.2	1.81	2.6	2.30±0.04
ϵ	78.4	92±5	106±18	79±8			97	98±8	121.6	79±5
τ_D (ps)	8.3		11±4	8			7.3		14.9	9.4±0.7
γ (dyn/cm)	72.0	52.7			92±5					66.9±0.9
$\Delta\phi$ (mV)		−500			−500					−540

[a]Molecular geometry from Ref. 52, μ_0 from Ref. 7, quadrupole from Ref. 96, dimer properties from Ref. 67, Δu from Ref. 59 using Eq. (3), D from Ref. 73, ϵ from Ref. 49, τ_D a consensus from Refs. 85–87.
[b]CHARMM version of the original TIP3P (Ref. 5). The liquid properties were computed from 10 simulations of 125 molecules in the isothermal–isobaric ensemble, using particle-mesh Ewald and a 9 Å Lennard-Jones cutoff. The surface tension γ and the surface potential $\Delta\phi$ are from Ref. 88.
[c]Reference 43. The diffusion constant D, the dielectric constant ϵ, and the Debye relaxation time τ_D are from Ref. 82.
[d]Reference 20. Constant volume simulations.
[e]Reference 19. The surface potential $\Delta\phi$ is from Ref. 91.
[f]Reference 21.
[g]Reference 46.
[h]Reference 47. The 5-site model has explicit lone pairs at $\ell_{OL}=0.5$ Å.
[i]Reference 48.
[j]This work.

yield bad liquid structure and bad self-diffusion constant. On the other hand, α cannot be freely adjusted to get correct $\langle v \rangle$ and Δu, because it has a major influence on the average dipole in the liquid, hence on the dielectric constant [see Fig. 3(b)]. From the vector diagrams of Fig. 3, it is clear that treating the molecular polarizability as a parameter removes some important collinearities and that the four parameters of the model provide altogether enough freedom to adjust all four target liquid properties.

The oxygen–oxygen, oxygen–hydrogen, and hydrogen–hydrogen radial distribution functions of the final model are shown in Fig. 4. The agreement with experimental radial distribution functions is generally excellent, which is in itself remarkable since no specific adjustments were made to reproduce this experimental data. The best models yielding good properties for the dimer and the average enthalpy and density naturally give reasonable liquid structure. The narrow shape of the first peak in the $g_{OO}(r)$ radial distribution function is probably due to the steepness of the Lennard-Jones repulsive potential and the lack of intramolecular flexibility. For the same reason, the first intramolecular peak of the $g_{OH}(r)$ distribution is slightly outward ($r_{OH}^{(1)}=1.85$ Å instead of 1.78 Å). The height of the first peak in the oxygen-oxygen radial distribution function is equal to 3.065. This value is somewhat high but almost within experimental errors ($g_{OO}^{(1)}=2.7\pm0.3$ from the neutron diffraction experiment[53]). The position and height of the first peak is necessary to match the experimental value of the self-diffusion constant in the liquid. It would be possible to reproduce the radial distribution function exactly by sacrificing the diffusion constant. Having $g_{OO}^{(1)}$ around 2.7 or lower gives $D>4\times10^{-5}$ cm^2/s, much higher than 2.3×10^{-5} cm^2/s, the experimental value.[73] In part, the intrinsic limitations of the conventional Lennard-Jones potential appear to be responsible for the inaccuracies of the average liquid structure. The harsh $1/r^{12}$ repulsion may not allow the position of the first peak in the oxygen–oxygen radial distribution function, $r_{OO}^{(1)}$, to differ significantly from d_{OO}, the oxygen–oxygen equilibrium distance in the water dimer. In the SWM4-DP model, d_{OO} is equal to 2.82 Å and the first peak is at 2.79 Å, smaller by only 0.03 Å. In contrast, while the position of the first peak determined experimentally is 2.73 Å, the equilibrium oxygen–oxygen distance in the water dimer is around 2.91 Å based on high level *ab initio* calculations,[74] perhaps even as large as 2.98 Å according to gas phase measurements.[67] This implies that there should be a shift on the order of 0.2 Å between $r_{OO}^{(1)}$ and d_{OO}. A softer repulsive potential may allow for such a difference to be reproduced. In the SWM4-DP model, both the large $r_{OO}^{(1)}$ and the relatively flat second peak

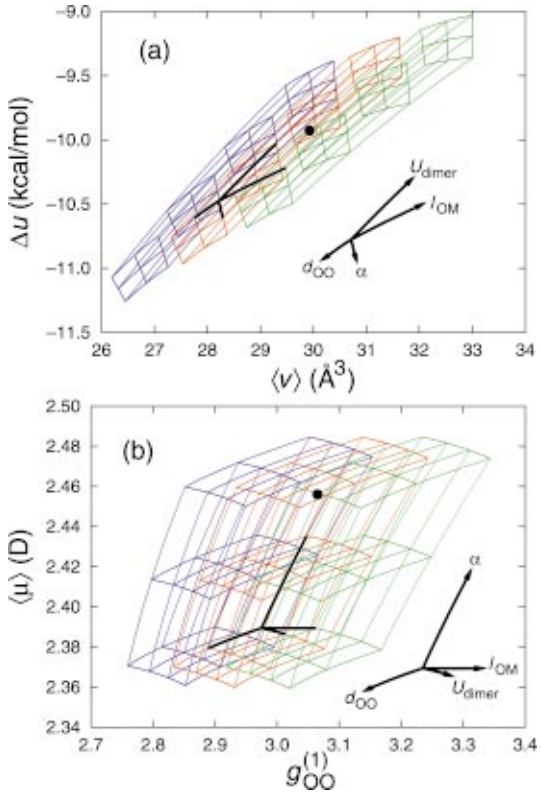

FIG. 3. (Color) Projections of the response surface $\mathbf{P}(\ell_{\mathrm{OM}},\alpha,U_{\mathrm{dimer}},d_{\mathrm{OO}})$ (a) in the $\langle v\rangle-\Delta u$ plane and (b) in the $g_{\mathrm{OO}}^{(1)}-\langle\mu\rangle$ plane: in blue for $\ell_{\mathrm{OM}}=0.23$ Å, in red for $\ell_{\mathrm{OM}}=0.24$ Å, and in green for $\ell_{\mathrm{OM}}=0.25$ Å. Each $3\times4\times3$ grid is showing how the properties are varying according to the three remaining parameters. The arrows show how to follow the grid for each parameter: $\alpha=0.95$, 1.00, 1.05 Å^3; $U_{\mathrm{dimer}}=-5.4,-5.3,-5.2,-5.1$ kcal/mol; and $d_{\mathrm{OO}}=2.81$, 2.82, 2.83 Å. The black dot shows the SWM4-DP liquid properties.

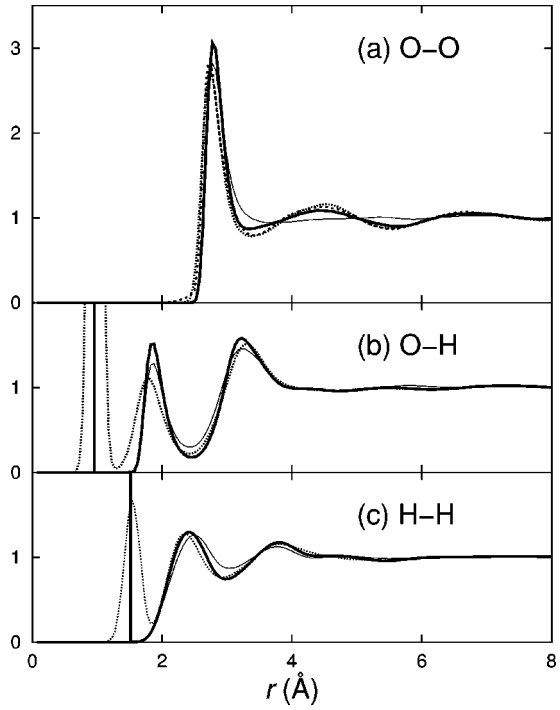

FIG. 4. (a) Oxygen–oxygen, (b) oxygen–hydrogen, and (c) hydrogen–hydrogen radial distribution functions for SWM4-DP (thick solid lines), compared to TIP3P distributions (thin solid lines) and experimental distributions: neutron diffraction data of Soper *et al.* (Ref. 53) for (a), (b), and (c) (dotted lines); x-ray diffraction data of Hura *et al.* (Ref. 54) for (a) (dashed lines).

of the $g_{\mathrm{OO}}(r)$ distribution are a necessary tradeoff to reproduce the diffusion constant. Nevertheless, the coordination number, defined as

$$N_{\mathrm{c}}=4\pi\rho\int_0^{r_{\mathrm{min}}}dr\,g_{\mathrm{OO}}(r), \tag{11}$$

is 4.63 for the SWM4-DP model (using $r_{\mathrm{min}}=3.35$ Å), in good agreement with the recent x-ray diffraction result of $N_{\mathrm{c}}=4.7$.[54,75]

The permanent dipole of the isolated molecule, μ_0, is set to exactly match the experimental gas phase value. The position of the M site is the only remaining free parameter which affects the permanent molecular quadrupole of an isolated molecule. But given the simplicity of the charge distribution, each individual component of the quadrupole cannot be reproduced exactly. Q_{xx} would be reproduced with $\ell_{\mathrm{OM}}=0.1789$ Å, Q_{yy} with $\ell_{\mathrm{OM}}=0.2642$ Å, and Q_{zz} with $\ell_{\mathrm{OM}}=0.2928$ Å. As shown in Table II, the optimal value of 0.23808 Å for ℓ_{OM} yields a reasonable compromise for each component of the molecular quadrupole, suggesting that a realistic molecular quadrupole is important for obtaining good liquid properties. This was also noted previously by Chialvo and Cummings.[76] Parenthetically, it may be noted that the present value of ℓ_{OM} is larger than for the TIP4P model (0.15 Å).[5] The TIP4P-FQ model,[20] a polarizable water model with charge transfer, left the distance ℓ_{OM} unchanged from its value in the TIP4P model. For the polarizable TIP4P-FQ model, this distance is perhaps suboptimal, since a larger distance of 0.23 yields a permanent quadrupole that is closer to the experimental value (see Table II). For the SWM4-DP model, a larger ℓ_{OM} also improves the hydrogen bond geometry of the water dimer. The acceptor angle θ_{A} is 70° instead of 27° for TIP4P-FQ,[20] closer to the experimental value $58\pm6°$.[67] This 70° may be a little too high, as it makes the total dipole of the dimer, μ_{dimer}, smaller than the experimental value (see Table II). Such an open angle reproduces the tetrahedral geometry of hydrogen bonding in water and is likely to give a correct liquid structure. Indeed, the liquid structure of SWM4-DP shows a significant improvement over that of TIP3P (see Fig. 4): The $g_{\mathrm{OO}}(r)$ distribution has a distinct second peak and even a third peak, and the first intramolecular peak of the $g_{\mathrm{HH}}(r)$ distribution has the correct position ($r_{\mathrm{HH}}^{(1)}=2.43$ Å). These are two signs of a better tetrahedral structure.

The polarizability of the optimal model is 1.04 Å^3, significantly smaller than the value of 1.44 Å^3 in the gas phase. Although this observation is undoubtedly dependent on the details of the present model, it is strongly supported by a very thorough exploration of the parameter space. Figure 5 shows how the dielectric constant is related to the average molecular dipole. This trend was initially displayed by Sprik,[9–11,77] from which it was concluded that an average dipole about 2.4 to 2.6 D was needed to correctly reproduce ϵ using classical molecular dynamics simulations. The

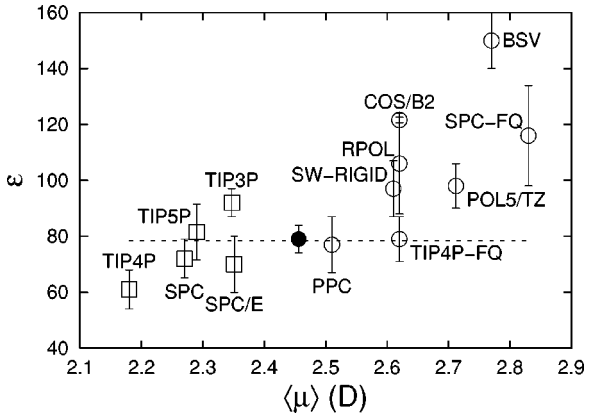

FIG. 5. Dielectric constants for selected water models. Nonpolarizable models (squares): TIP4P (Refs. 5 and 97), SPC (Refs. 6 and 97), TIP5P (Ref. 80), TIP3P (Ref. 5) (ϵ computed by the authors), and SPC/E (Ref. 97). Polarizable models (circles): SWM4-DP (this work, full circle), PPC (Ref. 45), SW-RIGID (Ref. 46), TIP4P-FQ (Ref. 20), RPOL (Refs. 43 and 82), COS/B2 (Ref. 48), POL5/TZ (Ref. 47), BSV (Ref. 44), and SPC-FQ (Ref. 20). Values with no reported uncertainties were assigned ± 10. The horizontal line shows the experimental value $\epsilon = 78.4$.

SWM4-DP model has $\langle \mu \rangle = 2.456$ D, a value smaller than that of any other polarizable model, although still within the broad range indicated by *ab initio* or density functional Car–Parrinello simulations on small water boxes: from 2.43 (Ref. 77) to 3.0 D.[12] An unequivocal value of $\langle \mu \rangle$ is difficult to calculate from a pure quantum mechanical approach because there is no unique way to partition the electronic density among the molecules. In addition, the computational cost of the method makes it difficult to simulate a bulk liquid during a time sufficiently long to sample many representative conformations. Hybrid quantum mechanical/molecular mechanical (QM/MM) descriptions seem to yield intermediate dipole values: 2.90 D for a quantum water molecule surrounded by four classical molecules placed in a spherical dielectric cavity,[78] and 2.71 D for a quantum water molecule surrounded by polarizable classical molecules.[79] Interestingly, consistent values are obtained from *ab initio* calculations using liquid conformations obtained from classical simulations of the TIP3P model[5] or the TIP5P model:[80] 2.65 (Ref. 71) and 2.60 ± 0.14 D,[81] respectively. A gas-phase-like α yields overestimated average dipole and dielectric constant. For example, the RPOL model,[43,82] with a permanent dipole of 2.024 D and a polarizability of 1.47 Å^3, and the SW-RIGID model,[46] with $\mu_0 = 1.85$ and $\alpha = 1.47$ Å^3, have both high dielectric constants (see Table II). In contrast, the TIP4P-FQ model[20] ($\mu_0 = 1.85$ D and $\alpha = 1.123$ Å^3), the PPC model[45] ($\mu_0 = 2.14$ and $\alpha = 0.56$ Å^3), and the present SWM4-DP model ($\mu_0 = 1.85$ D and $\alpha = 1.04$ Å^3) all have correct dielectric constants (see Fig. 5). Therefore, the fact that a reduced molecular polarizability is essential to reproduce the dielectric constant of the liquid appears to be a robust conclusion of the current effort. It is likely that this condensed-phase renormalization of the polarizability arises from the energy cost of overlapping electronic clouds due to Pauli's exclusion principle and that it should apply to other polar molecules.

The average molecular dipole $\langle \mu \rangle = 2.456$ D in a bulk liquid of SWM4-DP water molecules comprises the permanent dipole 1.85 D, plus an induced dipole of 0.606 D. With the current choice of spring constant to attach the Drude particle to the oxygen, this corresponds to a displacement of about 0.07 Å, away from the oxygen site toward the M site. Because of the symmetry of the molecule, the average induced dipole is parallel to the MO axis.

The TIP4P-FQ, SW-RIGID, and SWM4-DP models have very similar electrostatic properties (same permanent gas-phase dipole and same geometry), but have contrasting features that suggest why correct dielectric constants can be obtained for diverse average dipoles $\langle \mu \rangle$ (SWM4-DP versus TIP4P-FQ), and why similar average dipoles can produce different dielectric constants (TIP4P-FQ versus SW-RIGID). Both SWM4-DP and TIP4P-FQ have correct dielectric constants but, while the SWM4-DP model has a perfectly isotropic polarizability ($\alpha_x = \alpha_y = \alpha_z = 1.04$ Å^3), the TIP4P-FQ model (a charge-transfer model) has a very anisotropic molecular polarizability ($\alpha_x = 0.82$ Å^3, $\alpha_y = 2.55$ Å^3, $\alpha_z = 0$ Å^3) and a small molecular quadrupole compared with the experimental gas-phase (see Table II). The SW-RIGID model, on the other hand, produces the same average dipole as TIP4P-FQ, but has a nonrenormalized, isotropic polarizability. Its electrostatics differs from SWM4-DP mostly because of a larger α, which explains the larger average dipole and the larger dielectric constant. Ultimately, these differences are creating specific tetrahedral arrangements[83] and specific orientational fluctuations[84] that have an impact on the value of the dielectric constant.

The Debye relaxation time of the SWM4-DP model is 9.4 ± 0.7 ps, in reasonable agreement with the experimental values 8.27[85] 8.32[86] and 8.40 ps.[87] This result was obtained by fitting a single exponential to an average of the 20 autocorrelation functions $\Phi(t)$ for t between 0 and 40 ps.

B. Interfacial properties

Nonpolarizable water models with effective constant dipole may be reasonably valid for representing the interactions between molecules immersed in the bulk region, where they are assumed to be uniformly polarized by their surrounding. Because such nonpolarizable models are designed and optimized to reproduce the average properties of an isotropic bulk liquid, their inability to represent markedly anisotropic environments is expected to be limited. Such a nonisotropic environment is, perhaps, well-exemplified in the case of the vacuum-liquid interface. For this reason it is of interest to examine the properties of the vacuum-liquid interface with the SWM4-DP model.

The surface tension extracted from the five slab simulations of 1000 ps each is 66.9 ± 0.9 dyn/cm. This value compares well with the experimental surface tension of 72.0 dyn/cm and constitutes an improvement over the TIP3P model, that has a surface tension of 52.7 dyn/cm.[88] The anisotropic orientation of the water molecules at the interface gives rise to a nonzero electrostatic potential difference between the vacuum and the liquid. Figure 6 shows the interfacial potential across the z axis, $z = 0$ being the position of the center of mass of the water slab. As a test charge crosses the air/liquid interface (i.e., as z goes from -13 to -6 Å),

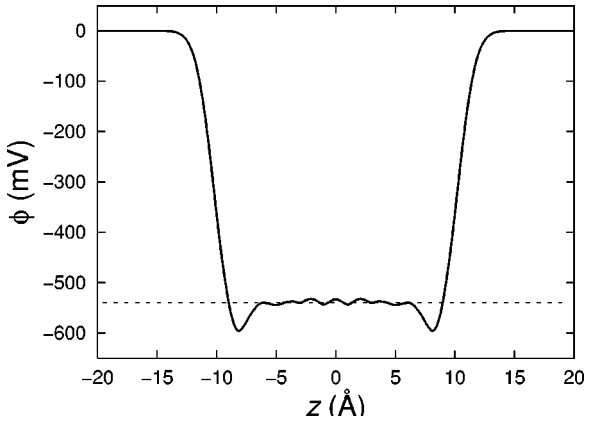

FIG. 6. Interfacial potential for the SWM4-DP model. The potential drop $\Delta\phi$ is represented by a dashed line at -540 mV.

the potential profile displays a rapid drop from $\phi=0$ to $\phi=-540$ mV. This potential drop reflects the average inward ordering of the molecular dipoles at the surface of the slab.[89] The interfacial potential $\Delta\phi$ cannot be measured directly, and experimental propositions for its magnitude—even for its sign—vary greatly (see Ref. 90 and references therein). For the present model, we get $\Delta\phi=-540$ mV, in good agreement with the nonpolarizable TIP3P and TIP4P models[5] (-500 mV[88] and -500 mV,[91] respectively) and with the polarizable POL model (-500 mV).[91] In contrast to these models, the SWM4-DP model displays a notable potential well at $z=-8$ Å (see Fig. 6). At this position, the interface has essentially the density of bulk water (data not shown), but the SWM4-DP molecules still display a significant orientational order. The order parameter $\langle\rho(z)\cos\theta(z)/\rho_{\text{bulk}}\rangle$,[88] where θ is the angle between the $\overrightarrow{\text{MO}}$ directors and the normal to the interface, has a significant negative value for z between -11 and -6 Å (with an extremum -0.08 at $z=-8.5$ Å). This indicates that the oxygen atoms at the interface are pointing toward the gas phase, in agreement with recent *ab initio* simulations.[92]

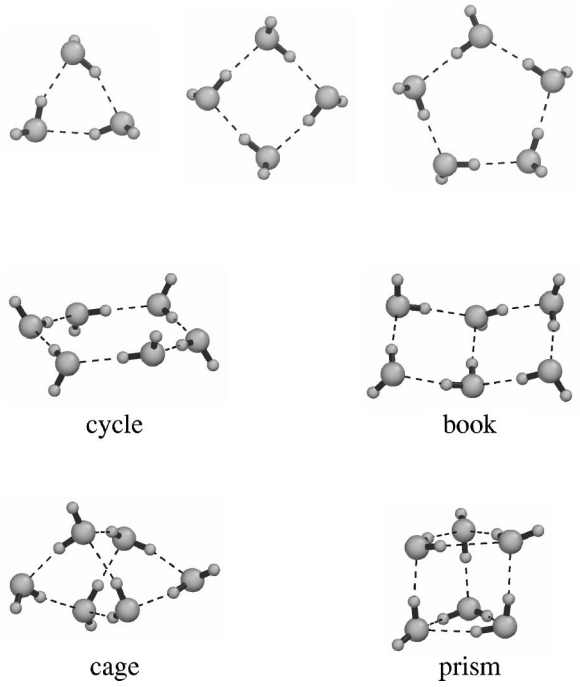

FIG. 7. Illustration of the SWM4-DP water clusters reported in Table III. For clarity, the M sites are not shown.

C. Water clusters

Although the SWM4-DP model is optimal for the bulk liquid properties, we expect the energetics of small water clusters ($N=3$ to 6) to be significantly better than with a nonpolarizable model like TIP3P.[5] The total binding energies of SWM4-DP clusters are presented in Table III for the cyclic trimer, cyclic tetramer, cyclic pentamer, and some standard hexamers: cycle, book, cage, and prism. Each of the hexamers has a definite hydrogen-bond topology but has many distinct stable conformers defined by how each water molecule participates in the hydrogen bonding. In Table III and Fig. 7, we report only the lowest-energy SWM4-DP conformers.

The binding energies of the SWM4-DP clusters are

TABLE III. Binding energies for water clusters. N_{Hb} is the number of hydrogen bonds. Energies in parentheses refer to a conformer different from the SWM4-DP conformer.

N	Isomer	N_{Hb}	*Ab initio*[a]	TIP3P[b]	TIP4P-FQ[c]	MCDHO[d]	POL5/TZ[c]	SWM4-DP[e]
3	cycle	3	−15.8	−17.75	−12.58	−13.98	−13.42	−14.44
4	cycle	4	−27.6	−29.47	−23.64	−25.86	−25.53	−25.22
5	cycle	5	−36.3	−38.91	−32.95	−35.30	−34.11	−33.43
6	cycle	6	−44.8	−47.64	−41.37	−44.26	−41.79	−41.27
6	book	7	−45.6	−48.23	−40.15	(−43.98)	−42.46	−42.62
6	cage	8	(−45.8)	−47.45	(−39.30)	−43.69	(−41.78)	−43.26
6	prism	9	−45.9	−46.69		(−44.12)		−42.96

[a]From Ref. 93.
[b]CHARMM version of the original TIP3P (Ref. 5). The lowest-energy TIP3P conformers are equivalent to those found for SWM4-DP, except for the trimer and tetramer being flat.
[c]From Ref. 47.
[d]From Ref. 21.
[e]This work.

systematically less negative than the *ab initio* results of Xantheas *et al.*[93] (MP2 theory converged to the complete basis set limit), also presented in Table III. This problem seems common for polarizable water models (see Table III): TIP4P-FQ[20] and POL5/TZ[47] were optimized for liquid properties, and are significantly less negative than SWM4-DP for the cage and prism isomers. The MCDHO model[21] was parametrized from *ab initio* data for the dimer and is better for small water clusters, but has inferior liquid properties. The problem is opposite for the nonpolarizable TIP3P model,[5] where the enhanced charges overestimate the stability of the water clusters. For the SWM4-DP model, the deviation from *ab initio* becomes smaller—per hydrogen bond—as the water molecules are more coordinated, that is, as the cluster is more representative of bulk water. Because each molecule is accepting only one hydrogen bond, the cyclic SWM4-DP clusters have the largest discrepancies: 0.45 kcal/mol/H-bond for the trimer, 0.60 kcal/mol/H-bond for the tetramer, 0.58 kcal/mol/H-bond for the pentamer, and 0.59 kcal/mol/H-bond for the cyclic hexamer. The errors on the hexamer binding energies decrease for more compact structures: 0.43 kcal/mol/H-bond for the book isomer, 0.32 kcal/mol/H-bond for the cage isomer, and 0.33 kcal/mol/H-bond for the prism isomer. Apparently, the renormalized polarizability of the SWM4-DP model is not optimal for molecules with less than four nearest neighbors. For rigid molecules, not allowed to relax the OH bond lengths and HOH bond angles, a smaller renormalization factor would be more appropriate. Indeed, a modified version of SWM4-DP with a nonrenormalized polarizability $\alpha = 1.44$ Å^3 gives significantly lower energies for the equivalent structures: -15.56 kcal/mol for the trimer, -28.19 kcal/mol for the tetramer, -38.42 kcal/mol for the pentamer, -48.24 kcal/mol for the cyclic hexamer, -48.52 kcal/mol for the book hexamer, -47.89 kcal/mol for the cage hexamer, and -47.68 kcal/mol for the prism hexamer. A challenge would be to design a model able to capture the progressive renormalization of α in increasingly large clusters, but that is beyond the scope of the present effort.

In agreement with recent *ab initio* studies,[93,94] the SWM4-DP model designates a nonplanar hexamer structure (a cage conformer) as the global energy minimum. This is contrasting with other polarizable models, such as TIP4P-FQ,[20] MCDHO,[21] and POL5/TZ,[47] that give planar global minima (see Table III). This is an important quality of the SWM4-DP model because the water hexamer is the smallest cluster for which the global energy minimum has a nonplanar hydrogen-bond topology.[8] The hexamer binding energy sequence for the SWM4-DP model is also consistent with *ab initio*:[93,94] $E_{\text{prism}} \approx E_{\text{cage}} < E_{\text{book}} < E_{\text{cycle}}$. The global SWM4-DP energy minimum corresponds to the cage structure illustrated in Fig. 7, and E_{cage} is actually 0.30 kcal/mol less than E_{prism}. The optimal SWM4-DP cage structure is equivalent to the reported *ab initio* cage (du){1} conformer of Losada and Leutwyler.[94] The second most stable SWM4-DP structure, at only 0.12 kcal/mol higher in energy, is equivalent to the *ab initio* cage conformer reported by Xantheas *et al.*[93] [(uu){1} according to Gregory and Clary's nomenclature[95]]. The third most stable structure is the prism conformer, followed by the book structure (see Table III and Fig. 7). Thus, although there is a small systematic underestimation of the water cluster binding energies, the relative energies are in good agreement with high-level *ab initio* data.

IV. CONCLUSION

The proposed water model uses Drude polarizability as the only new ingredient. It keeps a point-charge electrostatic representation and the common Lennard-Jones potential between the oxygen atoms. This simple polarizable model provides the essential electrostatics to reproduce the properties of the liquid phase at room temperature and pressure: the gas-phase molecular dipole (1.85 D), a good molecular quadrupole, and a smaller renormalized molecular polarizability.

The model uses an effective value of 1.04 Å^3 for the molecular polarizability, smaller than the experimental gas phase value of 1.44 Å^3. Such a renormalized value, which reflects the influence of the microscopic factors opposing polarization in the condensed phase, is necessary to obtain accurate properties of the liquid. This implies that the model retains some empirical character, i.e., some parameters are set to effective values designed to yield optimal properties for the liquid. It may be possible to design more realistic models by introducing some short range interactions between induced dipoles to account for the microscopic factors opposing polarization in the condensed phase. Nonetheless, this may not be necessary for our purpose. In the same spirit as the previous generation of nonpolarizable models with effective interactions,[2] it can be realistically hoped that simple models with an effective renormalized polarizability can accurately simulate biomolecular systems. Nonpolarizable models, in which the permanent dipole of the isolated molecule has been enhanced to simulate the bulk phase reasonably well,[5,6] owe much of their success to the fact that an effective dipole makes sense in most relevant situations because the polarity of the environment is similar. In the current polarizable model, that aspect of reality is accurately simulated, i.e., the correct permanent dipole can be attributed to the isolated molecule and the enhanced polarization arises naturally in the bulk phase. However, the polarizability is reduced and set to an effective empirical value. Nevertheless, such models can represent a wide range of situations accurately since the microscopic factors giving rise to the reduction in the molecular polarizability of a molecular moiety (Pauli's exclusion principle and the overlap of electronic clouds) may be assumed to have a similar effect in most dense systems.

The SWM4-DP model uses point charges and Lennard-Jones potentials because they are simple and give satisfactory properties. The optimal SWM4-DP model indicates that the ''12-6'' Lennard-Jones potential gives rise to a hard repulsion that cannot correctly reproduce both the oxygen–oxygen distance in the dimer, d_{OO}, and the position of the first peak in the oxygen–oxygen pair correlation function, $r_{\text{OO}}^{(1)}$. The SWM4-DP model compromises on both: d_{OO} is 2.82 Å instead of 2.91 Å[74] and $r_{\text{OO}}^{(1)}$ is 2.79 Å instead of 2.73 Å.[53,54] Moreover, to get a correct self-diffusion constant, the SWM4-DP model somewhat compromises on the liquid

structure: having $r_{OO}^{(1)}$ closer to the experimental value would have improved both the position and the amplitude of the second peak of the oxygen–oxygen radial distribution, but would have yielded a less diffusive liquid, and the $g_{OO}^{(1)}$ would have been even larger. To get a correct dielectric constant, the SWM4-DP model needs a relatively small average condensed-phase dipole and significant adjustment of the molecular polarizability. Some of these compromises could probably be alleviated by adopting a rigid molecular geometry adapted to the condensed phase, but the largest contribution is most likely due to the overall shape of the short-range and midrange interactions. For these reasons, we conclude that it might be worth considering alternative, *softer* interactions such as the Buckingham ''exp-6'' potential instead of Lennard-Jones potential and smeared charges instead of point charges in future models of water. In order to keep a correct self-diffusion constant along with a closer and lower first $g_{OO}(r)$ peak, such ''softer'' models should allow the oxygen atoms to move more freely within the first hydration shell.

The SWM4-DP model is optimal for the purpose of carrying classical molecular dynamics or Monte Carlo simulations of bulk solvent systems at room temperature and pressure. It may not yield accurate results if nonclassical effects arising from the quantum nature of the nuclei were taken into account explicitly, e.g., using simulations based on discretized Feynmann path integral.[41] Accordingly, it may need to be reparametrized if the internal geometry was allowed to be flexible. The SWM4-DP model has a simple functional form, yet it accurately reproduces the essential properties of liquid water under normal conditions. This makes it well suited for simulating the hydration of charged or highly polar molecules, including large biomolecules.

ACKNOWLEDGMENTS

B.R. is supported by NSF Grant No. 0110847. A.D.M. is supported by NIH Grant No. GM51501. Helpful discussions with R. Friesner and B. Berne are gratefully acknowledged. G.L. is grateful to Alain Caillé for his support.

[1] *Computational Biochemistry and Biophysics*, edited by O. M. Becker, A. D. MacKerell, Jr., B. Roux, and M. Watanabe (Marcel Dekker, New York, 2001).
[2] A. D. MacKerell, Jr., in *Computational Biochemistry and Biophysics*, edited by O. M. Becker, A. D. MacKerell, Jr., B. Roux, and M. Watanabe (Marcel Dekker, New York, 2001), Chap. 2.
[3] T. A. Halgren and W. Damm, Curr. Opin. Struct. Biol. **11**, 236 (2001).
[4] S. W. Rick and S. J. Stuart, in *Reviews in Computational Chemistry*, edited by K. B. Lipkowitz and D. B. Boyd (Wiley-VCH, Hoboken, NJ, 2002), Vol. 18, pp. 89–146.
[5] W. L. Jorgensen, J. Chandrasekhar, J. D. Madura, R. W. Impey, and M. L. Klein, J. Chem. Phys. **79**, 926 (1983).
[6] H. J. C. Berendsen, J. P. M. Postma, W. F. van Gunsteren, and J. Hermans, in *Intermolecular Forces*, edited by B. Pullman (Reidel, Dordrecht, 1981), pp. 331–342.
[7] T. R. Dyke and J. S. Muenter, J. Chem. Phys. **59**, 3125 (1973).
[8] J. K. Gregory, D. C. Clary, K. Liu, M. G. Brown, and R. J. Saykally, Science **275**, 814 (1997).
[9] M. Sprik, J. Chem. Phys. **95**, 6762 (1991).
[10] J.-C. Soetens, M. T. C. M. Costa, and C. Millot, Mol. Phys. **94**, 577 (1998).
[11] A. Wallqvist and R. D. Mountain, in *Molecular Models of Water: Derivation and Description*, Vol. 13 of *Reviews in Computational Chemistry*, edited by K. B. Lipkowitz and D. B. Boyd (Wiley-VCH, New York, 1999), Chap. 4, pp. 183–247.
[12] P. L. Silvestrelli and M. Parrinello, Phys. Rev. Lett. **82**, 3308 (1999).
[13] P. L. Silvestrelli and M. Parrinello, J. Chem. Phys. **111**, 3572 (1999).
[14] Y. S. Badyal, M.-L. Saboungi, D. L. Price, S. D. Shastri, D. R. Haeffner, and A. K. Soper, J. Chem. Phys. **112**, 9206 (2000).
[15] A. V. Gubskaya and P. G. Kusalik, J. Chem. Phys. **117**, 5290 (2002).
[16] I.-F. Kuo and D. J. Tobias, J. Phys. Chem. B **105**, 5827 (2001).
[17] C. J. Burnham, J. Li, S. S. Xantheas, and M. Leslie, J. Chem. Phys. **110**, 4566 (1999).
[18] M. W. Feyereisen, D. Feller, and D. A. Dixon, J. Phys. Chem. **100**, 2993 (1996).
[19] L. X. Dang and T.-M. Chang, J. Chem. Phys. **106**, 8149 (1997).
[20] S. W. Rick, S. J. Stuart, and B. J. Berne, J. Chem. Phys. **101**, 6141 (1994).
[21] H. Saint-Martin, J. Hernández-Cobos, M. I. Bernal-Uruchurtu, I. Ortega-Blake, and H. J. C. Berendesen, J. Chem. Phys. **113**, 10899 (2000).
[22] Y.-P. Liu, K. Kim, B. J. Berne, R. A. Friesner, and S. W. Rick, J. Chem. Phys. **108**, 4739 (1998).
[23] T. P. Lybrand and P. A. Kollman, J. Chem. Phys. **83**, 2923 (1985).
[24] M. Sprik, M. L. Klein, and K. Watanabe, J. Phys. Chem. **94**, 6483 (1990).
[25] L. X. Dang and D. E. Smith, J. Chem. Phys. **99**, 6950 (1993).
[26] S. J. Stuart and B. J. Berne, J. Phys. Chem. **100**, 11934 (1996).
[27] D. J. Tobias, P. Jungwirth, and M. Parrinello, J. Chem. Phys. **114**, 7036 (2001).
[28] S. S. Xantheas and L. X. Dang, J. Phys. Chem. **100**, 3989 (1996).
[29] R. A. Bryce, M. A. Vincent, N. O. J. Malcolm, I. H. Hillier, and N. A. Burton, J. Chem. Phys. **109**, 3077 (1998).
[30] O. M. Cabarcos, C. J. Weinheimer, J. M. Lisy, and S. S. Xantheas, J. Chem. Phys. **110**, 5 (1999).
[31] J. Baik, J. Kim, D. Majumdar, and K. S. Kim, J. Chem. Phys. **110**, 9116 (1999).
[32] W. H. Robertson, E. G. Diken, E. A. Price, J.-W. Shin, and M. A. Johnson, Science **299**, 1367 (2003).
[33] F. C. Lightstone, E. Schwegler, R. Q. Hood, F. Gygi, and G. Galli, Chem. Phys. Lett. **343**, 549 (2001).
[34] I. Bakó, J. Hutter, and G. Pálinkás, J. Chem. Phys. **117**, 9838 (2002).
[35] A. Wallqvist, Chem. Phys. Lett. **165**, 437 (1990).
[36] K. A. Motakabbir and M. L. Berkowitz, Chem. Phys. Lett. **176**, 61 (1991).
[37] A. Kohlmeyer, W. Witschel, and E. Spohr, Chem. Phys. **213**, 211 (1996).
[38] I.-C. Yeh and M. L. Berkowitz, J. Chem. Phys. **112**, 10491 (2000).
[39] M. H. New and B. J. Berne, J. Am. Chem. Soc. **117**, 7172 (1995).
[40] S. W. Rick and B. J. Berne, J. Phys. Chem. B **101**, 10488 (1997).
[41] R. A. Kuharski and P. J. Rossky, Chem. Phys. Lett. **103**, 357 (1984).
[42] P. Drude, *The Theory of Optics* (Longmans, Green, and Co., New York, 1902), translation by C. Riborg Mann and Robert A. Millikan.
[43] L. X. Dang, J. Chem. Phys. **97**, 2659 (1992).
[44] J. Brodholt, M. Sampoli, and R. Vallauri, Mol. Phys. **86**, 149 (1995).
[45] I. M. Svishchev, P. G. Kusalik, J. Wang, and R. J. Boyd, J. Chem. Phys. **105**, 4742 (1996).
[46] P. J. van Maaren and D. van der Spoel, J. Phys. Chem. B **105**, 2618 (2001).
[47] H. A. Stern, F. Rittner, B. J. Berne, and R. A. Friesner, J. Chem. Phys. **115**, 2237 (2001).
[48] H. Yu, T. Hansson, and W. F. van Gunsteren, J. Chem. Phys. **118**, 221 (2003).
[49] D. P. Fernandez, Y. Mulev, A. R. H. Goodwin, and J. M. H. L. Sengers, J. Phys. Chem. Ref. Data **24**, 33 (1995).
[50] W. F. Murphy, J. Chem. Phys. **67**, 5877 (1977).
[51] G. Lamoureux and B. Roux, J. Chem. Phys. **119**, 3025 (2003).
[52] *Water: A Comprehensive Treatise*, edited by F. Franks (Plenum, New York, 1972), Vol. 1: The Physics and Physical Chemistry of Water.
[53] A. K. Soper, F. Bruni, and M. A. Ricci, J. Chem. Phys. **106**, 247 (1997).
[54] G. Hura, J. M. Sorenson, R. M. Glaeser, and T. Head-Gordon, J. Chem. Phys. **113**, 9140 (2000).
[55] G. J. Martyna, D. J. Tobias, and M. L. Klein, J. Chem. Phys. **101**, 4177 (1994).
[56] G. J. Martyna, M. E. Tuckerman, D. J. Tobias, and M. L. Klein, Mol. Phys. **87**, 1117 (1996).
[57] B. R. Brooks, R. E. Bruccoleri, B. D. Olafson, D. J. States, S. Swaminathan, and M. Karplus, J. Comput. Chem. **4**, 187 (1983).
[58] T. Darden, D. York, and L. Pedersen, J. Chem. Phys. **98**, 10089 (1993).
[59] G. Jancsó and W. A. van Hook, Chem. Rev. **74**, 689 (1974).
[60] M. Neumann and O. Steinhauser, Chem. Phys. Lett. **106**, 563 (1984).
[61] A. D. Buckingham, Proc. R. Soc. London, Ser. A **238**, 235 (1956).

[62] M. Neumann and O. Steinhauser, Chem. Phys. Lett. **102**, 508 (1983).
[63] M. P. Allen and D. J. Tildesley, *Computer Simulation of Liquids* (Clarendon, Oxford, 1987).
[64] J. G. Kirkwood and F. P. Buff, J. Chem. Phys. **17**, 338 (1949).
[65] K. Ichikawa, Y. Kameda, T. Yamaguchi, H. Wakita, and M. Misawa, Mol. Phys. **73**, 79 (1991).
[66] M. Karplus, Acc. Chem. Res. **35**, 321 (2002).
[67] T. R. Dyke, K. M. Mack, and J. S. Muenter, J. Chem. Phys. **66**, 498 (1977).
[68] L. A. Curtiss, D. J. Frurip, and M. Blander, J. Chem. Phys. **71**, 2703 (1979).
[69] A. Morita and S. Kato, J. Chem. Phys. **110**, 11987 (1999).
[70] M. in het Panhuis, P. L. A. Popelier, R. W. Munn, and J. Ángyán, J. Chem. Phys. **114**, 7951 (2001).
[71] Y. Tu and A. Laaksonen, Chem. Phys. Lett. **329**, 283 (2000).
[72] A. Morita, J. Comput. Chem. **23**, 1466 (2002).
[73] K. Krynicki, C. D. Green, and D. W. Sawyer, Discuss. Faraday Soc. **66**, 199 (1978).
[74] M. P. Hodges, A. J. Stone, and S. S. Xantheas, J. Phys. Chem. A **101**, 9163 (1997).
[75] J. M. Sorenson, G. Hura, R. M. Glaeser, and T. Head-Gordon, J. Chem. Phys. **113**, 9149 (2000).
[76] A. A. Chialvo and P. T. Cummings, J. Chem. Phys. **105**, 8274 (1996).
[77] L. D. Site, A. Alavi, and R. M. Lynden-Bell, Mol. Phys. **96**, 1683 (1999).
[78] S. Chalmet and M. F. Ruiz-López, J. Chem. Phys. **115**, 5220 (2001).
[79] T. D. Poulsen, P. R. Ogilby, and K. V. Mikkelsen, J. Chem. Phys. **116**, 3730 (2002).
[80] M. W. Mahoney and W. L. Jorgensen, J. Chem. Phys. **112**, 8910 (2000).
[81] K. Coutinho, R. C. Guedes, B. J. C. Cabral, and S. Canuto, Chem. Phys. Lett. **369**, 345 (2003).
[82] D. E. Smith and L. X. Dang, J. Chem. Phys. **100**, 3757 (1994).
[83] P. Höchtl, S. Boresch, W. Bitomsky, and O. Steinhauser, J. Chem. Phys. **109**, 4927 (1998).
[84] B. Guillot, J. Mol. Liq. **101**, 219 (2002).
[85] U. Kaatze, J. Chem. Eng. Data **34**, 371 (1989).
[86] J. Barthel, K. Bachhuber, R. Buchner, and H. Hetzenauer, Chem. Phys. Lett. **165**, 369 (1990).
[87] J. T. Kindt and C. A. Schmuttenmaer, J. Phys. Chem. **100**, 10373 (1996).
[88] S. E. Feller, R. W. Pastor, A. Rojnuckarin, S. Bogusz, and B. R. Brooks, J. Phys. Chem. **100**, 17011 (1996).
[89] M. C. Goh, J. M. Hicks, K. Kemnitz, G. R. Pinto, T. F. Heinz, K. B. Eisenthal, and K. Bhattacharyya, J. Phys. Chem. **92**, 5074 (1988).
[90] M. Paluch, Adv. Colloid Interface Sci. **84**, 27 (2000).
[91] L. X. Dang and T.-M. Chang, J. Phys. Chem. B **106**, 235 (2002).
[92] P. Vassilev, C. Hartnig, M. T. M. Koper, F. Frechard, and R. A. van Santen, J. Chem. Phys. **115**, 9815 (2001).
[93] S. S. Xantheas, C. J. Burnham, and R. J. Harrison, J. Chem. Phys. **116**, 1493 (2002).
[94] M. Losada and S. Leutwyler, J. Chem. Phys. **117**, 2003 (2002).
[95] J. K. Gregory and D. C. Clary, J. Phys. Chem. A **101**, 6813 (1997).
[96] J. Verhoeven and A. Dymanus, J. Chem. Phys. **52**, 3222 (1970).
[97] K. Watanabe and M. L. Klein, Chem. Phys. **131**, 157 (1989).